Han, Y., Caliebe, M., Hage, F., Ramasse, Q., Pristovsek, M., Zhu, T., Scholz, F., and Humphreys, C. (2016) Toward defect-free semi-polar GaN templates on pre-structured sapphire. Physica Status Solidi B: Basic Solid State Physics, 253(5), pp. 834-839.

There may be differences between this version and the published version. You are advised to consult the publisher's version if you wish to cite from it.

This is the peer reviewed version of the following article: Han, Y., Caliebe, M., Hage, F., Ramasse, Q., Pristovsek, M., Zhu, T., Scholz, F., and Humphreys, C. (2016) Toward defect-free semi-polar GaN templates on pre-structured sapphire. Physica Status Solidi B: Basic Solid State Physics, 253(5), pp. 834-839, which has been published in final form at http://dx.doi.org/10.1002/pssb.201552636. This article may be used for non-commercial purposes in accordance with Wiley Terms and Conditions for Self-Archiving.

http://eprints.gla.ac.uk/131179/

Deposited on: 9 November 2016

Enlighten – Research publications by members of the University of Glasgow
http://eprints.gla.ac.uk

Towards defect free semi-polar GaN templates on pre-structured sapphire

Yisong Han[*,1], Marian Caliebe[2], Fredrik Hage[3], Quentin Ramasse[3], Markus Pristovsek[1], Tongtong Zhu[1], Ferdinand Scholz[2], and Colin Humphreys[1]

[1] Department of Materials Science and Metallurgy, University of Cambridge, 27 Charles Babbage Road, Cambridge CB3 0FS, United Kingdom

[2] Institute of Optoelectronics, Ulm University, Albert-Einstein-Allee 45, 89081 Ulm, Germany

[3] SuperSTEM, STFC Daresbury Laboratories, Daresbury WA4 4AD, United Kingdom

The microstructure of semi-polar (11-22) GaN templates grown on pre-structured r-plane sapphire by MOVPE has been characterised by TEM. Cross-sectional observations indicate that defects are generated in three regions of the layers: threading dislocations at the inclined GaN/sapphire interface, basal plane stacking faults (BSFs) at the c^--wing, BSFs and threading dislocations at the coalescence between neighbouring GaN stripes. An in-situ SiN interlayer deposited at an early stage of the growth is shown to be effective in blocking the propagation of dislocations, which is mainly attributed to SiN formed on the c-plane rather than on the (11-22) plane. Si-doped marker layers have been used to study the evolution of the growth front before coalescence as a function of temperature. A high growth temperature is associated with the formation of highly faceted GaN stripes. Dislocations originally running along the c-direction are bent to the [11-20] direction driven by a progressing (11-22) facet. An efficient defect reduction is realized as a result of terminating these dislocations at voids partially defined by the (11-20) facet.

* Corresponding author: e-mail yh241@cam.ac.uk, yisong.han@gmail.com, Phone: +44(0)1223 767930

1 Introduction

There is a need for large-size, cost-effective and high-quality semi-polar GaN templates for the development of semi-polar GaN based light emitting diodes, which are promising to give an increased light emitting efficiency due to a reduction in the in-built electric fields arising from spontaneous and piezoelectrically generated polarization in the c-direction [1,2]. Bulk semi-polar substrates with a very low defect density can be produced by slicing from thick layers of c-plane GaN, which still have a limited commercial potential due their small size and high cost [3]. Semi-polar GaN can be grown directly by heteroepitaxy on other substrate materials, e.g. semi-polar (11-22) GaN on m-plane sapphire. However, such layers contain a very high density of defects including dislocations and basal plane stacking faults (BSFs), and defect reduction mechanisms commonly used on the c-plane growth have been shown to be not sufficiently effective [4]. Semi-polar templates have also been developed on pre-structured sapphire (patterned) substrates [5,6]. This approach involves an initial growth of GaN along the c-direction followed by a coalescence between adjacent GaN stripes to form a continuous semi-polar surface. Previous works have established that a very low defect density can be achieved on semi-polar (11-22) GaN layers grown by metal-organic vapour phase epitaxy (MOVPE) on pre-structured r-plane (10-12) sapphire substrates [7].

In this work, we provide a detailed microstructural characterisation of semi-polar (11-22) GaN layers grown by MOVPE on pre-structured r-plane sapphire using transmission electron microscopy (TEM). We focus on the study of the generation and propagation of defects as the growth progresses, and the impact of incorporating a SiN interlayer for dislocation reduction before coalescence and its microstructure on different facets. In addition, a series of Si-doped marker layers (MLs) were deposited at different stages of the growth, which provide important insight into the evolution of the GaN stripes before coalescence as a function of growth temperature.

2 Experimental

The cross-section of the investigated layers is illustrated in Figure 1. Trenches were etched along the a-direction of r-plane sapphire. The period of the trenches is 6 µm. The GaN growth was carried out in a low-pressure horizontal flow Aixtron-200/4 RF-HT reactor using the precursors of trimethylgallium (TMGa), trimethyl-aluminium (TMAl) and high purity ammonia (NH_3) [8]. Briefly, the growth started from an oxygen-doped AlN

nucleation layer, followed by a GaN buffer layer at about 1105°C. Then an in-situ SiN interlayer for dislocation reduction was deposited. The growth continued at 1025ºC to achieve a coalescence for a continuous surface.

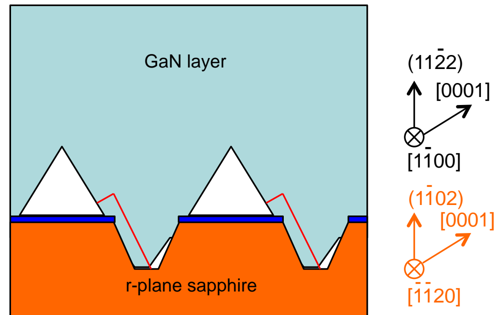

Figure 1 The general structure of the studied semi-polar GaN templates grown on pre-structured sapphire. The blue regions represent SiO_2 masks. The red lines represent a SiN interlayer deposited for dislocation reduction.

Cross-sectional TEM specimens were prepared by conventional mechanical polishing, followed by Ar ion beam milling. The GaN wafers were cut perpendicular to the trenches, enabling observations along the m-direction of GaN. The Ar ion beam milling was performed in a Gatan PIPS (Precision Ion Polishing System) at an angle of 7° and a voltage of 5 kV. The TEM samples were observed in a FEI Tecnai Orisis TEM/STEM 80-200 microscope. High-angle annular dark field (HAADF) scanning transmission electron microscopy (STEM) imaging was carried out using a Nion UltraSTEM100 electron microscope operated at 100 kV at the SuperSTEM laboratory, Daresbury, UK. The microscope has a Nion fifth-order spherical aberration corrector. HAADF-STEM images were recorded at a probe convergence semi-angle of 32.6 mrad and inner and outer collection angles of 76 and 185 mrad, respectively.

3 Results and discussion

3.1 Defect formation and development

Figure 2 shows a cross-sectional bright-field image taken from a sample containing a SiN interlayer deposited at a distance of ~1.5 μm from the c-plane-like GaN/sapphire interface. This image was recorded under a (11-24)

two-beam condition, in which all perfect dislocations, all Frank-Shockley partial dislocations and 2/3 Shockley partial dislocations are visible. The position of the SiN interlayer is marked by a white dashed line.

Three regions in the layer are of particular interest, as marked by the red rectangles. At Region A, where the growth starts, a high density of threading dislocations is generated at the inclined c-plane-like GaN/sapphire interface. These dislocations are bent by 90° towards either side of the c-direction. The dislocations bent downwards are terminated at the gaps in the trenches, whilst those bent upwards have chance to continue propagating towards the surface of the epilayer [5,9]. It is apparent that many dislocations are terminated by the SiN interlayer, suggesting a similar behaviour as that commonly used during the c-plane growth.

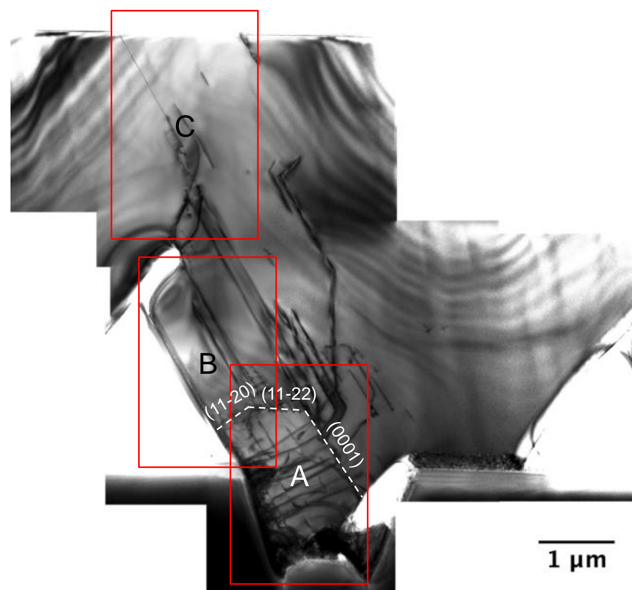

Figure 2 (11-24) two-beam bright-field image recorded close to the [1-100] zone axis showing one period of the patterned growth. A SiN interlayer is deposited (white dashed line) for dislocation reduction. Three regions of particular interest during the growth are marked by red rectangles. Region A is associated with the start of the growth of GaN on the inclined c-plane like sidewalls. Regions B and Region C are related to the c^--wing of the GaN stripes and the coalescence process between the neighbouring GaN stripes.

Region B is associated with the emerging of a c^--wing of the GaN layer and Region C with the coalescence between the adjacent GaN stripes. Figure 3 shows a dark-field image from a c^--wing and a bright-field image from a coalescence region of the GaN layer. Both images were recorded using a (1-100) two-beam condition, established after the TEM foil was tilted by 30º from the original [1-100] zone to one of the <11-20> zones. In

both cases, fringes due to the presence of planar defects are revealed, indicating BSFs are formed at these two regions. In addition, new threading dislocations are also generated at the coalescence point.

Overall, all three regions are associated with the generation of defects, i.e. threading dislocations at Region A and C, BSFs at Regions B and C. As demonstrated in Section 3.3, the propagation of these defects is strongly dependent of the growth conditions. Therefore, the growth needs to be well controlled to achieve a low defect density.

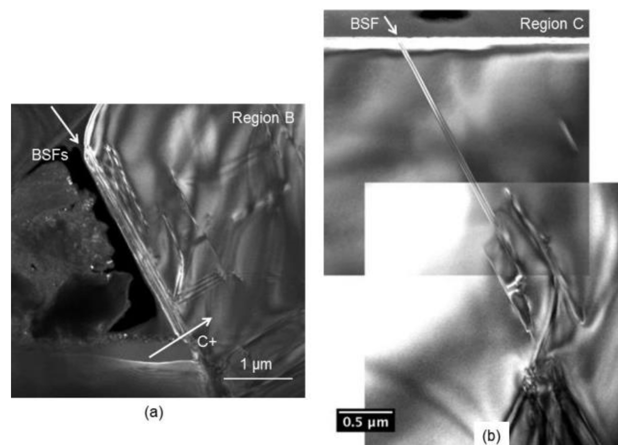

Figure 3 (a) (1-100) two-beam dark-field image taken from a c^--wing of a GaN stripe, corresponding to Region B in Figure 2. (b) (1-100) two-beam bright-field image taken from a coalescence region, corresponding to Region C in Figure 2. In both cases, fringes due to the presence of BSFs are revealed.

3.2 Dislocation reduction using a SiN interlayer

In our templates, a SiN interlayer was introduced at an early stage of the growth in order to block the propagation of dislocations towards the wafer surface. The position of a SiN interlayer with reference to the inclined GaN/sapphire interface, and its growth time and temperature has been studied in detail and reported elsewhere [8]. It is found that the crystal quality of the templates can be improved by a SiN interlayer deposited at certain growth conditions, as evidenced by X-ray diffraction and photoluminescence measurements.

Figures 4a,b show plan-view SEM-CL images from a wafer without a SiN interlayer and a wafer with SiN deposited after 7.5 min of the GaN growth. The corresponding cross-sectional dark-field TEM images are

presented in Figures 4c,d, recorded under a (11-22) two-beam condition. Apart from the dark spots which are correlated to threading dislocations, two sets of dark lines exist in the SEM-CL images. The angle between the dark lines and the in-plane [1-100] direction is 48º, corresponding to an intersection between the two inclined m-planes and the (11-22) growth surface. Higher magnification SEM-CL images revealed that these dark lines are composed of dark spots, indicating that they are dislocations clusters.

Similar dark lines were reported on very thin InGaN layers grown on free-standing (11-22) GaN substrates. They were identified by TEM as being misfit dislocations with a prismatic slip on the inclined m-planes [10]. However, the dark lines (or dislocation clusters) observed in this work are considered to be formed due to a preferential glide of pre-existing threading dislocations to some m-planes for stress relaxation [11].

Overall, the effect of the SiN interlayer is apparent since the density of dark lines as well as dark spots in Figure 4a is much less than those in Figure 4b, indicating a significant reduction in dislocation density. The cross-sectional TEM images qualitatively support the SEM-CL images, with Figure 4d contains much fewer dislocations in comparison with Figure 4c.

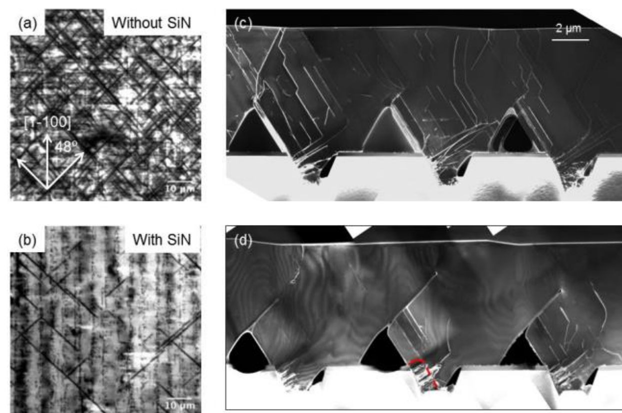

Figure 4 (a,b) Plan-view SEM-CL images collected from a wafer without a SiN interlayer and a wafer with a SiN interlayer. (c,d) Corresponding cross-sectional dark-field TEM images from these two samples. The position of the SiN interlayer in (d) is marked by a red dashed line.

As shown in Figure 2, at the time when the SiN interlayer is deposited, the growth front consists of three facets, i.e. the (0001), (11-22) and (11-20) facets. The area ratio between these three facets changes progressively with the growth, with the (11-22) facet eventually becoming dominant at the point of coalescence. It is well

documented in the literature that on the c-plane, Si acts as an anti-surfactant, and a stable monolayer structure with holes is formed [12]. Dislocation reduction is realized through either a direct blocking by the SiN mask or through an annihilation among dislocations passing through the holes in the SiN mask. However, SiN on the semi-polar (11-22) plane has been reported to be not as effective as that on the a- and c-plane [4]. In order to understand the very different behaviour of SiN on the semi-polar plane, (11-22) GaN templates on m-plane sapphire with a series SiN interlayers deposited with increasing growth time were prepared. The longest deposition time for SiN is searched until the GaN growth cannot recover after the SiN deposition. Cross-sectional Cs-corrected STEM imaging provides atomic-scale structural and chemical information from the SiN interlayers, which is difficult to achieve by other techniques. STEM images from SiN interlayers on the c-plane were also acquired for comparison.

Figure 5 shows HAADF-STEM images taken from a SiN interlayer on the c-plane (Figures 5a,b) and a SiN interlayer on the (11-22) plane (Figures 5c,d). All these images were recorded along the [1-100] zone axis. On the c-plane, the SiN interlayer indeed forms a monolayer structure with holes allowing the GaN growth to continue. It exhibits the fingerprint structure with a repetition of two bright atomic columns followed by a dark atomic column, in agreement with the configuration and structural model reported [12]. However, on the semi-polar (11-22) plane, only dark patches (lower intensity than the GaN matrix) appear. Electron energy loss spectroscopy (EELS) elemental mapping confirmed that the dark patches are Si-rich and slightly Ga-poor. However, there is no sign of SiN forming a continuous layer or/and a new lattice structure at all the growth times used. This suggests that SiN deposited on the (11-22) plane does not provide an effective dislocation blocking mechanism.

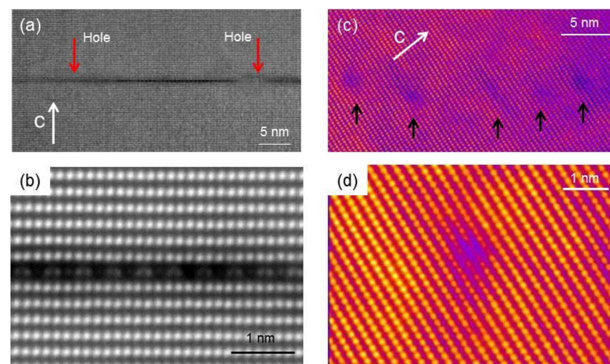

Figure 5 HAADF-STEM images taken from a SiN interlayer deposited (a,b) on the c-plane and (c,d) on the semi-polar (11-22) plane.

As discussed in the next section, a favourable growth condition to achieve a low defect density is to maintain all three facets before coalescence. Under such conditions, most dislocations bent at the very early stage of the growth to the [11-20] direction will be terminated at voids anyway between the neighbouring GaN stripes. Therefore, a SiN interlayer deposited close to the GaN/sapphire interface, when the c-plane facet is dominant and the (11-22) facet is relatively small, is recommended in order to maximise its effect on the c-plane for dislocation reduction.

3.3 Impact of GaN stripe shape on defect development

In order to achieve a better understanding of the development of GaN stripes with increasing growth temperature, and its impact on coalescence and defect structure of the GaN templates on patterned sapphire, a series of Si-doped marker layers were deposited at different stages of the growth. The general structure of these epilayers is illustrated in Figure 6. The growth of the samples in this section is slightly different from that of the previous ones. In this case, the growth is divided into three sections [13]. In GaN layer 1, the same procedure is used as mentioned in the experimental section including the deposition of a SiN interlayer. Then the growth continues for a short while at 1000°C before the temperature is set to either 950ºC or 1050ºC. Five Si-doped marker layers were deposited at this stage every 10 min. This was followed by layer 2 and layer 3 grown at 970ºC and 1040ºC, respectively.

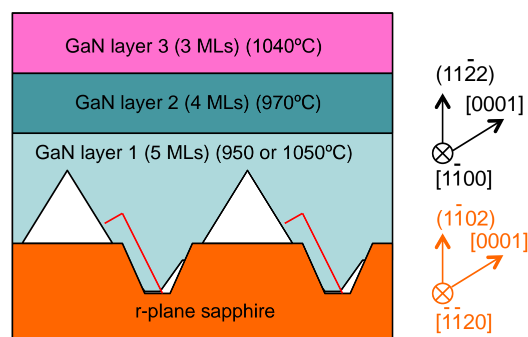

Figure 6 Structure of semi-polar GaN templates with Si-dope marker layers grown on pre-structured sapphire.

The first two rows in Figure 7 show cross-sectional SEM images and bright-field STEM images from the samples with GaN layer 1 grown at 950º and 1050ºC. A (11-24) two condition was established for STEM imaging and all threading dislocations are in contrast. Since the marker layers are not visible in the STEM images, their positions are redrawn according to those in the corresponding SEM images. The third row in Figure 7 shows panchromatic plan-view SEM-CL images from the two samples. For the 1050ºC sample, four facets, (0001), (11-22) (×2) and (11-20), co-exist during the growth of GaN layer 1. In comparison, a lower growth temperature results in a complete absence of the (11-20) facet and a very small (0001) facet. According to the SEM-CL images, a direct benefit from having many different facets formed at a higher growth temperature is a dramatically reduced defect density including both dislocations and BSFs. The dark spot densities are estimated to be ~3×10^{8} cm^{-2} for the 950º wafer and ~8×10^{7} cm^{-2} for the 1050ºC wafer.

It is noted that the samples shown in Figure 7 do not exhibit the dark lines, even though they are visible in Figure 4. Since all the templates studied in this work were grown under roughly the same conditions, we attribute the difference mainly to an improved processing of the trenches on sapphire and a change of their shapes. The new trenches (0.6 µm deep) are shallower than the older ones (1.1 µm deep). Their c-plane-like sidewalls are oriented closer to the sapphire c-plane (~55° instead of ~70°), i.e. the angle of the new sidewalls with reference to the (11-22) plane is closer to the ideal value of 58.4° [14]. The reduced depth of the trenches is associated with a smaller inclined GaN/sapphire interface and thereby less threading dislocations are generated at the start of the growth. The better orientation of the sidewalls is considered to be beneficial for the wafers to release strain built up during growth and then to reduce the driving force for the dislocations to glide to the m-planes.

Such a defect reduction is a combined effect of bending of dislocations originally running along the c-direction and terminating of defects propagating primarily with the (11-20) facet. Due to the absence of a low-index out-of-plane crystallographic direction for the semi-polar (11-22) growth, dislocations tend to bend towards a [11-20] direction, which is considered to be energetically favourable [15]. The bending of a threading dislocation is a dynamic process and occurs when it intersects with a progressing (11-22) plane. As shown in Figure 7c, dislocations can in fact bend either up or down, because of the presence of two {11-22} type facets, depending on which facet it first comes across. In the 1050º template, the existence of the larger (0001) facet allows plenty of dislocations to still propagate along the c-direction without bending since they have no chance to intersect

with a (11-22) facet. Once the growth of the (11-20) facet ends due to a blockage from the neighbouring GaN stripe or at the coalescence, the propagation of dislocations (dislocation line direction is [11-20]) and BSFs (formed at the c^--wing) associated with this facet is terminated. However, such a self-blocking mechanism does not exist in the 950º sample. In this case, all dislocations running along the [11-20] direction together with the BSFs formed at the c^--wing have good chance to penetrate to the wafer surface. Accordingly, the BSFs found on the surface of the 950º sample are considered to be dominated by those originating from the c^--wing rather than being formed during the coalescence [13]. However, the sample with the highly faceted GaN stripes grown at 1050º requires a longer coalescence time and is more likely to have cracks due to an unsuccessful coalescence.

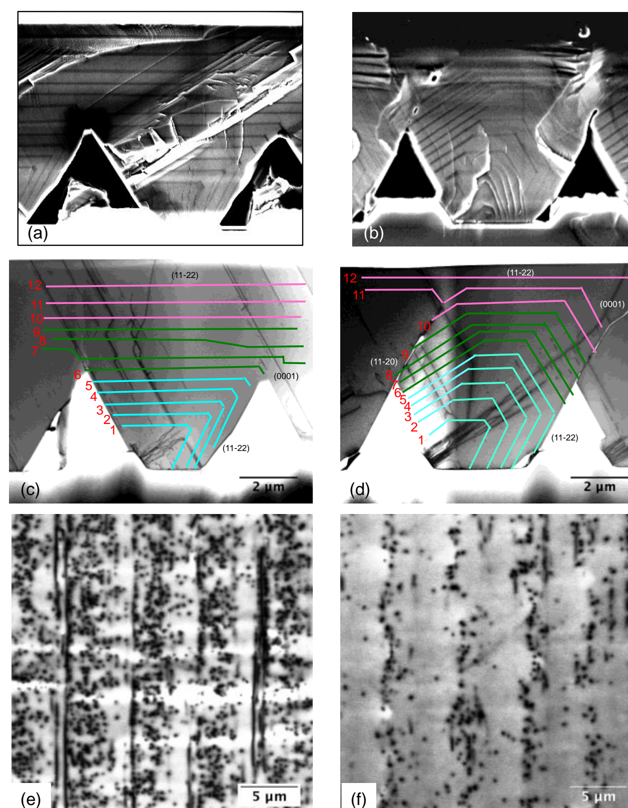

Figure 7 Images taken from wafers with a GaN layer 1 grown at 950ºC (left colunm) and 1050ºC (right column), respectively. (a,b) Cross-sectional SEM images, where the Si-doped GaN marker layers are visible. (c,d) Cross-sectional STEM bright-field images with the marker layers redrawn according to those in (a,b). The color of a marker layer indicates which GaN layers they belong to in Figure 6. (e,f) Panchromatic plan-view SEM-CL images.

Table 1 Comparison of density of defects reported in the literature and obtained from this work.

Ref.	Dislocation density (cm^{-2})	BSF density (cm^{-1})
Tendille, *et al.* [7]	5.1×10^{7}	30
Vennéguès, *et al.* [9]	7.0×10^{7}	70
Furuya, *et al.* [16]	1.3×10^{8}	-
de Mierry, *et al.* [17]	5.0×10^{8}	-
Our templates	8.5×10^{7}	~200

The use of voids associated a (11-20) facet has also been shown by other groups to be an efficient way of blocking the propagation of defects to the wafer surface [7,16,17]. Defect densities reported in the literature and obtained from our templates are listed in Table 1. Most of the results were obtained based on SEM-CL measurements. Accordingly, the patterned growth generally gives a dislocation density in the range between 10^{7} and 10^{8} cm^{-2} and a BSF density in the order of 10^{2} cm^{-1}. Since the detected BSFs are generated during the coalescence event and their density is already low, the chance for a further reduction based on the same patterning on sapphire through growth is low and even may not be necessary. Recently, additional measures mainly targeting dislocations have been taken. For example, before coalescence, a second selective growth on the (0001) and (11-20) facets of GaN stripes may be performed, leading to a homogenous distribution of dislocations [18]. In addition, the growth may start from a low temperature aiming for a broad (11-22) facet for dislocation bending, followed by a higher temperature promoting the formation of highly faceted GaN stripes [13]. Unfortunately, this can result in an overgrowth of the (11-20) facet, blocking the adjacent (0001) facet rather than being blocked [13]. As proposed by Vennéguès [9], a longer period of trenches on sapphire or/and an overgrowth by halide vapour phase epitaxy (HVPE) on top of a MOVPE layer may be used. However, according to our experiments, longer-period trenches require the growth of a thicker MOVPE layer to achieve a full coalescence and can result in a loss of growth selectivity [19]. In addition, a high density of surface hillocks is often observed on the surface of the HVPE layers grown on MOVPE GaN, a problem still waiting to be solved [20].

4 Conclusions

Cross-sectional TEM observations show that defects can be generated in three regions in semi-polar GaN layers grown on pre-structured sapphire substrates. They may all have chance to propagate to the wafer surface under certain growth conditions. An in-situ SiN interlayer has been used as an additional defect reduction method. Atomic resolution STEM images show that SiN deposited on the semi-polar plane does not form a new crystallographic structure, suggesting that it is not as effective as that on the c-plane.

Dislocations along the c-direction formed at the GaN/sapphire interface are bent by 90º to the [11-20] direction, driven by a progressing (11-22) facet. A high growth temperature before coalescence is essential for the formation of highly faceted GaN stripes and then to achieve a low defect density template. Most of these dislocations together with BSFs formed at the c^--wing are terminated at voids associated with the (11-20) facets.

Acknowledgements

We thank C. Steinmann and R. Rösch of the Institute of Optoelectronics at Ulm University for technical support. This work was financially supported by the European Commission (FP7) within the framework of the project "AlGaInN materials on semi-polar templates for yellow emission in solid state lighting applications" (ALIGHT) (Project No.: 280587) and by the Deutsche Forschungsgemeinschaft (DFG) within the framework of the project "Polarization Field Control in Nitride Light Emitters" (PolarCoN). SuperSTEM is the UK Engineering and Physical Sciences Research Council (EPSRC) National Facility for aberration-corrected STEM.

References

[1] J.-H. Ryou, P. D. Yoder, J. Liu, Z. Lochner, H. Kim, S. Choi, H. J. Kim and R. D. Dupuis, IEEE J. Sel. Top. Quant. Electron. **15** (4), 1080-1091 (2009).

[2] J. S. Speck and S. F. Chichibu, MRS Bull. **34** (05), 304-312 (2009).

[3] S. F. Chichibu, M. Kagaya, P. Corfdir, J.-D. Ganière, B. Deveaud-Plédran, N. Grandjean, S. Kubo and K. Fujito, Semicond. Sci. Technol. **27** (2), 024008 (2012).

[4] M. Pristovsek, M. Frentrup, Y. Han and C. J. Humphreys, Phys. Stat. Sol. B, n/a-n/a (2015).

[5] N. Okada, A. Kurisu, K. Murakami and K. Tadatomo, Appl. Phys. Express **2** (9), 091001 (2009).

[6] F. Scholz, T. Wunderer, B. Neubert, M. Feneberg and K. Thonke, MRS Bull. **34** (05), 328-333 (2009).

[7] F. Tendille, P. De Mierry, P. Vennéguès, S. Chenot and M. Teisseire, J. Cryst. Growth. **404**, 177-183 (2014).

[8] M. Caliebe, T. Meisch, B. Neuschl, S. Bauer, J. Helbing, D. Beck, K. Thonke, M. Klein, D. Heinz and F. Scholz, Phys. Stat. Sol. C **11** (3-4), 525-529 (2014).

[9] P. Vennéguès, F. Tendille and P. De Mierry, J. Phys. D: Appl. Phys. **48** (32), 325103 (2015).

[10] F. Wu, E. C. Young, I. Koslow, M. T. Hardy, P. S. Hsu, A. E. Romanov, S. Nakamura, S. P. DenBaars and J. S. Speck, Appl. Phys. Lett. **99** (25), 251909 (2011).

[11] N. Okada, A. Ishikawa, K. Yamane, K. Tadatomo, U. Jahn and H. Grahn, Phys. Stat. Sol. A **211** (4), 736-739 (2014).

[12] T. Markurt, L. Lymperakis, J. Neugebauer, P. Drechsel, P. Stauss, T. Schulz, T. Remmele, V. Grillo, E. Rotunno and M. Albrecht, Phys. Rev. Lett. **110** (3), 036103 (2013).

[13] M. Caliebe, Y. Han, M. Hocker, T. Meisch, C. Humphreys, K. Thonke and F. Scholz, Phys. Stat. Sol. B, n/a-n/a (2015).

[14] S. Schwaiger, S. Metzner, T. Wunderer, I. Argut, J. Thalmair, F. Lipski, M. Wieneke, J. Bläsing, F. Bertram and J. Zweck, Phys. Stat. Sol. B **248** (3), 588-593 (2011).

[15] P. Vennéguès, B. Beaumont, V. Bousquet, M. Vaille and P. Gibart, J. Appl. Phys. **87** (9), 4175-4181 (2000).

[16] H. Furuya, Y. Hashimoto, K. Yamane, N. Okada and K. Tadatomo, J. Cryst. Growth. **391**, 41-45 (2014).

[17] P. de Mierry, N. Kriouche, M. Nemoz and G. Nataf, Appl. Phys. Lett. **94** (19), 191903 (2009).

[18] F. Tendille, M. Hugues, M. Teisseire and P. De Mierry, Semicond. Sci. Technol. **30** (6), 065001 (2015).

[19] S. Schwaiger, PhD thesis, Ulm University, 2011.

[20] Y. Han, M. Caliebe, M. Kappers, F. Scholz, M. Pristovsek and C. Humphreys, J. Cryst. Growth. **415**, 170-175 (2015).